# Asphericity in Supernova Explosions from Late-Time Spectroscopy

Keiichi Maeda[1,2,3,*], Koji Kawabata[4], Paolo A. Mazzali[2,5,6], Masaomi Tanaka[7], Stefano Valenti[8,9], Ken'ichi Nomoto[1,6,7], Takashi Hattori[10], Jinsong Deng[11], Elena Pian[5], Stefan Taubenberger[2], Masanori Iye[12], Thomas Matheson[13], Alexei V. Filippenko[14], Kentaro Aoki[10], George Kosugi[15], Youichi Ohyama[16], Toshiyuki Sasaki[10], and Tadafumi Takata[17]

[1]Institute for the Physics and Mathematics of the Universe (IPMU), University of Tokyo, Kashiwa-no-ha 5-1-5, Kashiwa City, Chiba 277-8582, Japan

[2]Max-Planck-Institut für Astrophysik, Karl-Schwarzschild-Straße 1, 85741 Garching, Germany

[3]Department of Earth Science and Astronomy, College of Arts and Science, University of Tokyo, Tokyo 153-8902, Japan

[4]Hiroshima Astrophysical Science Center, Hiroshima University, Hiroshima 739-8526, Japan

[5]National Institute for Astrophysics-OATs, Via G.B.Tiepolo, 11, 34143 Trieste, Italy

[6]Research Center for the Early Universe, School of Science, University of Tokyo, Tokyo 113-0033, Japan

[7]Department of Astronomy, School of Science, University of Tokyo, Tokyo 113-0033, Japan,

[8]Physics Department, University of Ferrara, I-44100 Ferrara, Italy

[9]European Organization for Astronomical Research in the Southern Hemisphere, Karl-Schwarzschild-Straße 1, 85741 Garching, Germany

[10]Subaru Telescope, National Astronomical Observatory of Japan (NAOJ), 650 North A'ohoku Place, Hilo, HI 96720

[11]National Astronomical Observatory, CAS, 20A Datun Road, Chaoyang District, Beijing 100012, China

[12]Division of Optical and Infrared Astronomy, NAOJ, Osawa 2-21-1, Mitaka, Tokyo 181-8588, Japan

[13]National Optical Astronomy Observatory, Tucson, AZ 85719, USA

[14]Department of Astronomy, University of California, Berkeley, CA 94720-3411, USA

[15]ALMA Project, NAOJ, Mitaka, Tokyo 181-8588, Japan

[16]Department of Infrared Astrophysics, ISAS, Japan Aerospace Exploration Agency (JAXA), 3-1-1 Yoshinodai, Sagamihara, Kanagawa 229-8510, Japan

[17]Astronomy Data Center, NAOJ, Mitaka, Tokyo 181-8588, Japan

[*]To whom correspondence should be addressed; E-mail: maeda@ea.c.u-tokyo.ac.jp

**Core-collapse supernovae (CC-SNe) are the explosions that announce the death of massive stars. Some CC-SNe are linked to long-duration gamma-ray bursts (GRBs) and are highly aspherical. One important question is to what extent asphericity is common to all CC-SNe. Here we present late-time spectra for a number of CC-SNe from stripped-envelope stars, and use them to explore any asphericity generated in the inner part of the exploding star, near the site of collapse. A range of oxygen emission-line profiles is observed, including a high incidence of double-peaked profiles, a distinct signature of an aspherical explosion. Our results suggest that all CC-SNe from stripped-envelope stars are aspherical explosions and that SNe accompanied by GRBs exhibit the highest degree of asphericity.**

Massive stars ($M \gtrsim 10 M_\odot$) end their lives when the nuclear fuel in their innermost region is consumed; lacking sufficient internal pressure support, they can no longer withstand the pull of gravity. Their core then collapses to a neutron star or a black hole. Gravitational energy from the collapse produces an explosion that expels the rest of the star in what is observed as a supernova (SN).

Core-collapse SNe (CC-SNe) are classified (*1*) by how much of the stellar envelope is present at the time of the explosion (*2*). Stars that retained their hydrogen envelope produce SNe with a H-rich spectrum, classified as Type II. On the other hand, stars that have lost all, or most, of the H-envelope produce CC-SNe that are known as "stripped-envelope" (briefly "stripped") SNe. These include, in a sequence of increasing envelope stripping, Type IIb (He rich, but still showing some H), Type Ib (He-rich, no H), and Type Ic (deprived of both H and He). Some SNe Ic (hereafter "broad-lined" SNe Ic) show very broad absorption features in optical spectra obtained within a few weeks of the explosion; these features are produced by material moving at $v > 0.1c$ ($c$ is the speed of light), probably the result of an explosion characterized by a kinetic energy ($E_{\rm K}$) larger than the canonical value of $\sim 10^{51}$ erg (*3*). The most energetic broad-lined SNe Ic can reach $E_{\rm K} \gtrsim 10^{52}$ erg (hereafter "hypernovae" or "GRB-HNe") (*4*), and can be associated with gamma-ray bursts (GRBs) (*5*). Figure 1 summarizes the relation between $E_{\rm K}$ and the mass of $^{56}$Ni that powers the optical light of stripped CC-SNe (*6*).

An important unsolved question concerns how gravitational energy of the collapse is turned into outward motion of the SN explosion. Most recently proposed scenarios involve aspherical explosions (*7–11*). Therefore, mapping the explosion geometry can be illuminating. It is especially critical to establish whether the explosion geometry is similar for all CC-SNe, or at least for different subclasses (GRB-HNe, broad-lined SNe Ic, normal-energy SNe, or stripped vs. Type II SNe).

Some evidence for asymmetric explosions was obtained from the polarization detected in several SNe II (*12*) and SNe Ib/c (*13*), and in the broad-lined SN Ic 2002ap (*14–16*). However, as there are still few such detections, no systematic study exists.

The best way to investigate a supernova's inner ejecta geometry is through late-time spectroscopy. At $t \gtrsim 200$ days after the explosion, expansion makes the density of the ejecta so low that optical photons produced anywhere in the ejecta escape without interacting with the gas. At these epochs, the SN spectrum is nebular, showing emission lines mostly of forbidden transitions. Because the expansion velocity is proportional to radius of any point in the ejecta, the Doppler shift indicates where the photon was emitted: a photon emitted from the near/far side of the ejecta is detected at a shorter/longer (blueshifted/redshifted) wavelength. The late-time nebular emission profiles thus probe the distribution of the emitting gas within the SN ejecta. This strategy is particularly effective for stripped CC-SNe, since we can look directly into the oxygen core.

Analysis of the late-time spectra of the GRB-HN SN Ic 1998bw (*17*) and of the broad-lined SN Ic 2003jd (*18*) provided evidence that these objects shared a similar, bipolar explosion. However, we viewed SN 1998bw on-axis, and SN 2003jd sideways. This seems consistent with the fact that SN 1998bw was associated with a GRB, while SN 2003jd was not, and suggests that if SN 2003jd also produced a GRB, this was missed because of its orientation ((*18*), but see (*19*) for concerns).

We obtained late-time spectra of stripped CC-SNe to study their morphology and quantify their properties. Our data were obtained mostly with FOCAS (*20*) on the 8.2 m Subaru telescope and with FORS2 on the ESO Very Large Telescope (VLT). Additional data are from (*21*). The strongest emission line in stripped CC-SNe is [O I] $\lambda\lambda$6300, 6363. Despite being a doublet, it behaves like a single transition if the lines are sufficiently broad ($\gtrsim 0.01c$), because the red component is weaker than the blue one by a factor of 3 (see supporting online text).

Since at epochs larger than 200 days after the explosion the ejecta are transparent to line emission, and radiation transfer is unimportant (see supporting online text), we selected spectra obtained at least 200 days after discovery to build an unbiased data set. Additionally, we did not include hypernovae discovered through an associated GRB, to avoid bias in the viewing angle. The selection procedure and possible biases are discussed in (*22*). Our sample (Tab. S1) is the largest published data set to date of stripped CC-SNe at such late epochs. Figure 2 shows the spectra of the 18 SNe in our sample. Among them, 13 are presented here for the first time.

The observed [O I] $\lambda\lambda$6300, 6363 emission profiles can be compared with the prediction of various explosion models. We use three representative models from (*23*): one extremely aspherical (BP8), one mildly aspherical (BP2), and one spherical (BP1).

In the spherical model, $^{56}$Ni is confined in a central high-density region with an inner hole, and is surrounded by a low-density, oxygen-rich region (*24*). This results in a single-peaked, but flat-topped [O I] profile, independent of the orientation.

On the other hand, the bipolar model (*24–26*) is characterized by a low-density $^{56}$Ni-rich region located near the jet axis, where the jets convert stellar material (mostly oxygen) into Fe-peak elements, and by a high-density disk-like structure composed of unburned oxygen-rich material, as the jet expands laterally only weakly (*17, 24*) (see Fig. S1). The

[O I] profile in a bipolar model depends on both the degree of asphericity and the viewing angle (*23, 27*) (see supporting online text and Fig. S1). If a bipolar supernova explosion is viewed from a direction close to the jet axis, the O-rich material in the equatorial region expands in a direction perpendicular to the line of sight, and the [O I] emission profile is observed to be sharp and single-peaked. On the other hand, for a near-equatorial view the profile is broader and double-peaked. The best fit to the light curve and the spectra of the GRB-HN SN 1998bw was obtained with model BP8 (*23, 27*).

For the degree of asphericity of this model, the [O I] profile should switch from single- to double-peaked near a viewing angle $\theta \approx 50^\circ$ measured from the jet direction (Fig. S2). The predicted frequency of double-peaked [O I] is thus $\sim 64\%$, in the absence of bias in the orientation. For a less aspherical model the fraction of double peaks is reduced: model BP2 shows double peaks only for $\theta \gtrsim 70^\circ$, and has a double-peak fraction of $\sim 34\%$. With this variety of [O I] profiles, statistics (Tab. 1) can be used to constrain the degree of asphericity and remove the uncertainty in the viewing angle.

Figure 3 shows the [O I] emission profiles for our sample. Out of 18 SNe, 5 (SNe 2003jd, 2004fe, 2005aj, 2005kl, and 2006T) clearly show double-peaked [O I] profiles. Four others (SNe 1997dq, 2004gn, 2005kz, and 2005nb) are apparently transitional objects with flat-topped or mildly peaked [O I] profiles, and there is a marginal detection of double peaks in some cases. The remaining 9 SNe exhibit single-peaked profiles. For illustrative purposes, the observed profiles are compared with model predictions in Figure 3.

The line profiles are well reproduced by the bipolar explosion model assuming different viewing angles. Although detailed fits are not unique for individual objects, this uncertainty does not affect the bulk statistics (single- vs. double-peaked): the presence of double-peaked [O I] profiles is not predicted in spherical models, and their fraction yields a secure estimate of the number of aspherical SNe viewed sideways, assuming that the sample is unbiased in orientation. The high incidence of double-peaked profiles is an important discovery: double-peaked [O I] was previously reported only for SN Ic 2003jd (*18*) and SN Ib 2004ao (*28*). The observed fraction of double-peaked profiles, (5 to 9)/18 (= 28%–50%, median $\sim 39\%$) is consistent with all stripped CC-SNe being mildly aspherical, like model BP2.

On the other hand, the observed fraction does not support the possibility that all stripped CC-SNe are extremely aspherical explosions like SN 1998bw (i.e., model BP8), as then we would expect an even larger fraction of double-peaked [O I] profiles: according to our Monte Carlo simulations with randomly oriented viewing directions, the observed number should be $7-16$ out of 18 SNe with 99% confidence level and $10-13$ with 70% confidence level. Alternatively, about half of all stripped CC-SNe may have asphericity as large as that of GRB-HNe, with a double-peak incidence of $\sim 64\%$ (BP8), with the remaining half being approximately spherical and yielding the bulk of the single-peaked profiles. With a larger SN sample we could look in more detail at [O I] profiles as functions of the degree of asphericity and orientation, and more fully explore these scenarios.

Although our sample is still small, we can look for statistical differences between

GRB-HNe, broad-lined SNe Ic, and other stripped CC-SNe. In our sample, six SNe are broad-lined (non-GRB) SNe Ic (SNe 1997ef, 1997dq, 2002ap, 2003jd, 2005kz, and 2005nb), while the rest are probably "normal" stripped CC-SNe. The observed fraction of double-peaked [O I] is 33% (1 out of 3 SNe) for broad-lined SNe Ic and 36% (4 out of 11) for the others, if SNe with transitional [O I] profiles (Fig. 3) are excluded. Within the statistical uncertainty, caused especially by the small sample of broad-lined SNe Ic, there is no difference between the two groups. Both are consistent with the predictions of model BP2, and show too few double-peaked profiles for model BP8. This suggests that on average, broad-lined, non-GRB SNe Ic are less aspherical than GRB-HNe, and morphologically closer to normal stripped CC-SNe.

Broad-lined, non-GRB SNe Ic have typically smaller $E_{\rm K}$ than GRB-HNe (Fig. 1). There has been speculation that broad-lined, non-GRB SNe Ic might be intrinsically similar to GRB-HNe but viewed off-axis, leading to apparently smaller $E_{\rm K}$. Although this may still be true for a small subset of them, the moderate asphericity inferred for this group suggests that broad-lined, non-GRB SNe Ic are probably intrinsically different from GRB-HNe.

On the other hand, asphericity is not a special feature of GRB-HNe, but rather a generic property of stripped CC-SNe. Both broad-lined and normal stripped CC-SNe have a moderate degree of asphericity. All stripped CC-SNe probably share to some extent a common explosion mechanism that generates the same kind of asphericity, with GRB-HNe likely the most aspherical. Our result offers an important insight into the theory of SN explosions. The most popular models for high- and low-energy CC-SNe are in fact different: black hole formation and the production of a jet in hypernovae and perhaps broad-lined SNe Ic (*29*); delayed neutrino heating from the proto-neutron star for normal SNe (*30*). In the former case, the explosion is probably initiated along the axis of rotation and/or magnetic field (*10, 11, 29*), while in the latter case some asphericity may be generated by hydrodynamic instabilities (*7–9*). The result supports recent theoretical scenarios of the supernova explosion, which suggest that an important role in the collapse is played by hydrodynamic instability, rotation, or magnetic fields.

Recently, Modjaz et al. (*31*) showed another sample of late-time spectra of stripped CC-SNe. Their conclusions are similar to ours. One SN in their sample (SN 2004ao with double-peaked [O I]) could be added to our sample according to our selection criteria. It increases the frequency of double-peaked events, but it does not change our conclusions within the uncertainties.

## References and Notes


1. A. V. Filippenko, *Ann. Rev. Astron. Astrophys.* **35**, 309 (1997).

2. K. Nomoto, K. Iwamoto, & T. Suzuki, *Phys. Rep.* **256**, 173 (1995).

3. P. A. Mazzali, et al., *Astrophys. J.* **572**, L61 (2002).

4. K. Iwamoto, et al., *Nature* **395**, 672 (1998).

5. T. J. Galama, et al., *Nature* **395**, 670 (1998).

6. K. Nomoto, et al., *Il Nouvo Cimento* **121B**, 1207 (2007) (astro-ph/0702472).

7. J. M. Blondin, A. Mezzacappa, & C. DeMarino, *Astrophys. J.* **584**, 971 (2003).

8. R. Buras, H.-Th. Janka, M. Rampp, & K. Kifonidis, *Astronomy and Astrophysics* **457**, 281 (2006).

9. A. Burrows, E. Livne, L. Dessart, C. D. Ott, & J. Murphy *Astrophys. J.* **655**, 416 (2007).

10. K. Kotake, H. Sawai, S. Yamada, & K. Sato, *Astrophys. J.* **608**, 391 (2004).

11. S. G. Moiseenko, G. S. Bisnovatyi-Kogan, & N. V. Ardeljan, *Mon. Not. Roy. Astron. Soc.* **370**, 501 (2006).

12. D. C. Leonard, et al., *Nature* **440**, 505 (2006).

13. L. Wang, D. A. Howell, P. Höflich, & J. C. Wheeler, *Astrophys. J.* **550**, 1030 (2001).

14. K. S. Kawabata, et al., *Astrophys. J.* **580**, L39 (2002).

15. D. C. Leonard, A. V. Filippenko, R. Chornock, & R. J. Foley, *Publ. Astron. Soc. Pacific* **114**, 1333 (2002).

16. L. Wang, D. Baade, P. Höflich, & J. C. Wheeler, *Astrophys. J.* **592**, 457 (2003).

17. K. Maeda, et al., *Astrophys. J.* **565**, 405 (2002).

18. P. A. Mazzali, et al., *Science* **308**, 1284 (2005).

19. A. M. Soderberg, E. Nakar, E. Berger, & S. R. Kulkarni, *Astrophys. J.* **638**, 930 (2006).

20. N. Kashikawa, et al., *Publ. Astron. Soc. Japan* **54**, 819 (2002).

21. T. Matheson, A. V. Filippenko, W. Li, D. C. Leonard, & J. C. Shields, *Astronomical J.* **121**, 1648 (2001).

22. Data and Methods are available as supporting online materials on Science Online.

23. K. Maeda, K. Nomoto, P. A. Mazzali, & J. Deng, *Astrophys. J.* **640**, 854 (2006).

24. K. Maeda & K. Nomoto, *Astrophys. J.* **598**, 1163 (2003).

25. A. M. Khokhlov, P. A. Höflich, E. S. Oran, J. C. Wheeler, L. Wang, & A. Yu. Chtchelkanova, *Astrophys. J.* **524**, L107 (1999).

26. A. I. MacFadyen, S. E. Woosley, & A. Heger, *Astrophys. J.* **550**, 410 (2001).

27. K. Maeda, P. A. Mazzali, & K. Nomoto, *Astrophys. J.* **645**, 1331 (2006).

28. M. Modjaz, et al., *Astron. J.* **in press** (2008) (astro-ph/0701246).

29. A. I. MacFadyen & S. E. Woosley, *Astrophys. J.* **524**, 262 (1999).

30. H. A. Bethe & J. R. Wilson, *Astrophys. J.* **295**, 14 (1985).

31. M. Modjaz, R.P. Kirshner, P. Challis, preprint (2008) (astro-ph/0801.0221)

32. The data were collected at the Subaru Telescope (the National Astronomical Observatory of Japan). The additional data were from the Very Large Telescope (European Southern Observatory) under ESO Program 078.D-0246. K.M. and M.T. have been supported by the Japan Society for the Promotion of Science (JSPS). E.P. and P.M. acknowledge financial support from PRIN MIUR 2005 and from PRIN INAF 2006. K.N. is supported by the JSPS Grant-in-Aid for Scientific Research (18104003, 18540231). J.D. is supported by NSFC (No. 10673014). A.V.F. is supported by NSF grant AST–0607485.

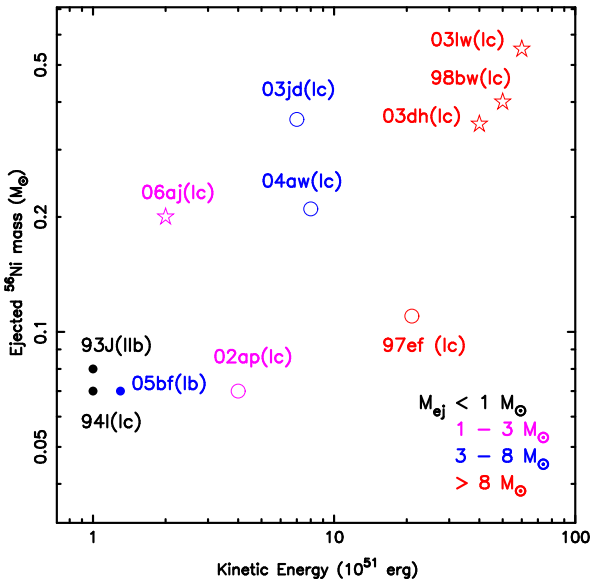


Figure 1: Relation between the kinetic energy of the explosion ($E_{\rm K}$) and the mass of ejected $^{56}$Ni [$M(^{56}{\rm Ni})$] of stripped CC-SNe (see supporting online text). Colors indicate the ejecta mass ($M_{\rm ej}$). For SN IIb 1993J and SN Ib 2005bf, the ejecta mass after subtracting the He envelope mass is shown as $M_{\rm ej}$, to compare with SNe Ic, which lack the He envelope. SNe associated with GRBs or an X-ray flash (XRF) are indicated by stars, and broad-lined SNe Ic without GRBs/XRFs by open circles. Other (normal) stripped CC-SNe are shown as dots.

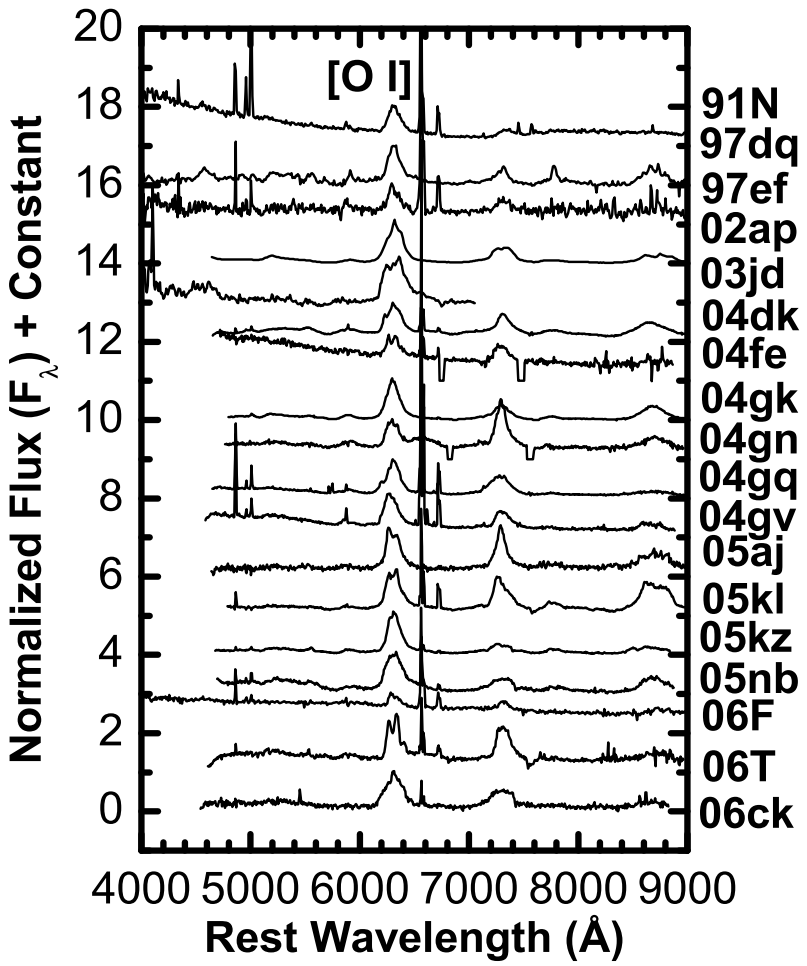


Figure 2: Nebular spectra of the supernovae in the sample used in this study. Narrow lines (e.g., H$\alpha$ at 6563 Å) originate from a diffuse superposed H II region, not from a SN. The spectra of SNe 1991N, 1997dq, 1997ef are from (*21*). The other spectra were obtained with the Subaru telescope, except for SN 2006F which was taken by the VLT (*22*). Spectra were deredshifted using the redshift obtained from the observed wavelength of the narrow H$\alpha$ emission if possible; otherwise, the redshift of the nucleus of the host galaxy was adopted. For presentation, the flux is arbitrarily scaled and shifted vertically. The strongest emission line (dashed line) is [O I] $\lambda\lambda$6300, 6363. The feature at $\sim 7,300$ Å is [Ca II] $\lambda\lambda$7291, 7324 contaminated by several emission lines: [O II], [Fe II], and [Ni II].

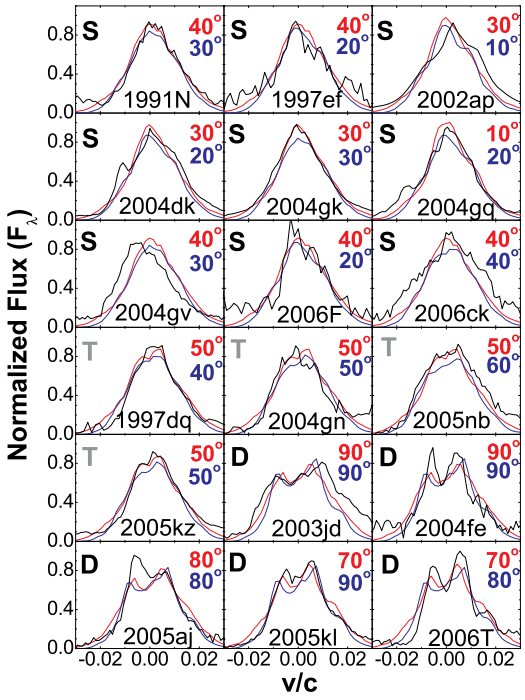


Figure 3: Observed [O I] $\lambda\lambda$6300, 6363 emission-line profiles (black curves), classified into characteristic profiles: single peaked (denoted by "S," top 9 SNe), transition ("T," middle 4 SNe), and double peaked ("D," bottom 5 SNe). For presentation, model predictions of the bipolar model (*23*) with different viewing directions are shown for Model BP8 (red curves, with the direction denoted by the red text) and for the less aspherical model BP2 (blue). The models shown here have smaller expansion velocities (corresponding to $E_{\rm K} \approx$ a few $\times 10^{51}$ erg) than the one applied to SN 1998bw ($E_{\rm K} \gtrsim 10^{52}$ erg) (*23*). The separation between the two peaks in the double-peaked cases is $\sim 0.01c - 0.02c$, much larger than the wavelength resolution in the observations ($\sim 10$ Å, corresponding to $0.0015c$).

Table 1: Fraction of double-peaked [O I] SNe.

| Model | Dividing angle[1] | Fraction[2] |
|---|---|---|
| Spherical | — | 0% |
| BP2 | $\sim 70^\circ$ | $\sim 34\%$ |
| BP8 | $\sim 50^\circ$ | $\sim 64\%$ |
| Observed | — | $39 \pm 11\%$ |

[1]The viewing angle ($\theta_0$ measured from the jet direction) which divides the [O I] profile — i.e., single peaked if $\theta < \theta_0$ and double peaked if $\theta_0 \leq \theta \leq 90^\circ$.
[2]Fraction of SNe showing double-peaked [O I].

# SUPPORTING ONLINE MATERIAL

Asphericity in Supernova Explosions from Late-Time Spectroscopy

Keiichi Maeda et al.

## Data and Methods

**Sample of Supernova Nebular Spectra:**
In the years 2005 to early 2007, we obtained a number of spectra of stripped CC-SNe using the 8.2 m Subaru telescope equipped with FOCAS. We also obtained several spectra using the VLT with FORS2 from late 2006 to early 2007. Some of the spectra are distinctly nebular, while others are not. In addition to this new sample, we include some spectra presented in (*S1*), which contains the largest sample of previously published late-time spectra of stripped CC-SNe. The spectral resolution is $\sim 10$ Å for the spectra obtained by the Subaru or VLT. The spectra from the previous sample (*S1*) were obtained with the Shane 3-m reflector at Lick Observatory, with similar spectral resolution (6–15 Å).

Because of the faintness of SNe in the late phases, the spectra can be obtained only for relatively bright SNe even with the largest telescopes in the world. The limiting functions are thus the intrinsic luminosity and the distance. The luminosity bias may be important when interpreting the data if the effect is strong: our sample then represents a subclass of luminous SNe (i.e., SNe with a large amount of $^{56}$Ni), and may affect the asymmetry statistics we investigate in the present paper.

However, we believe that the effect is not strong enough to affect our interpretation. First, our criterion for successful spectroscopy is $\sim 23$ mag. This roughly corresponds to SNe with a peak magnitude of 17 or 18. This brightness is similar to the criterion for obtaining high-quality data with typical SN observations in the early phases using smaller telescopes. As such, our sample should not be very different from samples of well-studied stripped CC-SNe in past studies using early-phase observations which, for example, led to the result shown in Figure 1. Second, the peak luminosity of very luminous stripped CC-SNe is larger than that of typical ones by at most a factor of $\sim 5$ (e.g., SN 1998bw (*S2*)), so the detection volume of these luminous events is larger than that of typical ones by at most one order of magnitude. However, the intrinsic rate of the very luminous events is probably smaller than that of the typical ones by nearly two orders of magnitude (*S3*). Thus, contamination by very luminous SNe should not be large in our sample. Finally, there is a correlation between the $^{56}$Ni mass and the early-phase width of absorption lines (*S4*). Using this relation, we indeed divide our sample into a potentially luminous class (i.e., broad-lined SNe Ic) and the other ones in the discussion of the asphericity statistics. Also, according to past studies, normal stripped CC-SNe (i.e., not broad-lined SNe Ic) have similar $^{56}$Ni mass ($\sim 0.1 M_\odot$) and represent a wide range of progenitor masses up to $\sim 20 M_\odot$ (*S4*). This suggests that the luminosity bias, if present, is not strong in the

normal stripped CC-SNe. In summary, the luminosity bias should not be strong in our sample of late-time spectra. Thus, the distance is probably the limiting factor, and our data consist of SNe within a distance of at most $\sim 100$ Mpc.

Other possible biases are (1) a possibility of preferentially observing SNe from a special direction (e.g., a jet axis), and (2) contamination of SNe which are young and dense so that their ejecta are not sufficiently transparent to trace the geometry by the [O I] profile. Here we describe how we selected the final unbiased list of supernova spectra expected to be at a fully nebular epoch to study the intrinsic line profile (Table S1).

First, we excluded SNe 1998bw, 2003dh, 2005bf, and 2006aj. SN Ic 2006aj was associated with an X-Ray flash (XRF: a low-energy analog of a GRB) (*S5*); thus, the detection of SN 2006aj is probably biased by the viewing-angle effect, being easier for an observer along the jet direction. For the same reason, we excluded SNe 1998bw and 2003dh, associated with GRB 980425 and GRB 030329, respectively, although there are some published late-phase observations for these objects (*S6, S7*). SN Ib 2005bf is reported to be a very peculiar SN, whose explosion mechanism may be different from that of typical CC-SNe; the nebular observations are found to be peculiar, too (*S8*). Observations and analyses of SN 2006aj and SN 2005bf in nebular phases are described in separate papers (*S8–10*). Note that in the late-time phases considered here, the dependence of luminosity on the viewing angle is negligible.

Next, we excluded supernovae which were observed only at times before entering the fully nebular phase, since optical transport effects can change the line profile. The choice is not trivial; the optical depth ($\tau$) differs for different supernovae ($\tau \propto M_{\rm ej}^2/E_{\rm K}$), and the ejecta mass ($M_{\rm ej}$) and the ejecta kinetic energy ($E_{\rm K}$) are not known a priori. The uncertainty in the explosion date further complicates matters.

Therefore, we applied a very simple criterion. We checked the phases of the observations with respect to the discovery date ($t$), and selected a supernova only if it was observed at $t > 200$ days at least once. Thus, any SNe possibly younger than 200 days were excluded from the list. This criterion, $t > 200$ days, is sufficiently late so that any selected supernova is certainly in the nebular phase.

Following these procedures, we obtained the unbiased sample of stripped CC-SNe whose spectra are distinctly nebular. The sample contains 18 SNe. One of the SNe is of Type IIb. The sample contains 13 SNe newly observed (11 only by the Subaru telescope, and 2 both by the Subaru and VLT). Spectra of two broad-lined SNe Ic (2002ap and 2003jd) were also obtained with the Subaru telescope, which were already reported (*S11, S12*). The remaining 3 SNe are from the previously published sample of (*S1*). In terms of the spectral characteristics in the early phase, 6 SNe in our list have been classified as broad-lined SNe Ib/c without association with a GRB (SNe 1997dq, 1997ef, 2002ap, 2003jd, 2005kz, and 2005nb – see also Figure 1 in the main text).

In cases where the supernova was observed at multiple epochs, we included the object in the nebular sample if the last observation satisfied the condition $t > 200$ days. Such SNe were used to check the validity of the selection criterion. SN 2005aj was observed

at three epochs ($t$ = 189, 249, and 312 days), showing significant evolution of the [O I] $\lambda\lambda$6300, 6363 profile between the first two epochs. SN 2006F was observed at $t$ = 173 and 312 days, showing no noticeable evolution in the [O I] profile. The other SNe observed multiple times at $t \gtrsim 200$ days do not show noticeable evolution in the [O I] profile. These observations justify our criterion ($t > 200$ days).

All the spectra shown in Figures 2 and 3 in the main text are at $t > 200$ days except for that of SN 2005nb. The signal-to-noise ratio for the spectrum of SN 2005nb at $t$ = 403 days is low, but the [O I] profile does not evolve significantly from $t$ = 195 days (shown in Figures 2 and 3 in the main text).

## Supporting Text

**The properties of stripped CC-SNe: $E_{\rm K}$, $M(^{56}{\rm Ni})$, and $M_{\rm ej}$:**
The kinetic energy of the explosion ($E_{\rm K}$), the mass of $^{56}$Ni [$M(^{56}{\rm Ni})$], and the ejecta mass ($M_{\rm ej}$) shown in Figure 1 of the main text are derived by modeling the early-phase observations using approximate analytical expressions (SNe 2003jd and 2004aw) or one-dimensional radiation transport codes (the other SNe). An exception is SN Ib 2005bf, for which $M(^{56}{\rm Ni})$ is derived by modeling the late-time observations (*S8*).

Assuming spherical symmetry, the estimate of $E_{\rm K}$ (shown in Figure 1) represents an isotropic value, which could be different from the intrinsic value by up to a factor of a few. For example, for SN 1998bw (associated with GRB 980425), we estimated $E_{\rm K} \approx 5 \times 10^{52}$ erg with a spherical model (*S2*), but $E_{\rm K} \approx 2 \times 10^{52}$ erg with a two-dimensional jet model (*S13*). The difference can be attributed to a viewing-angle effect. Since SN 1998bw is an extreme case (see the main text), the difference between the isotropic value and the real one should be smaller for other SNe.

The references are as follows: SN IIb 1993J (*S14*), SN Ic 1994I (*S15*), SN Ic 1997ef (*S16*), SN Ic 1998bw (*S2*), SN Ic 2002ap (*S17*), SN Ic 2003dh (*S18*), SN Ic 2003jd (*S19*), SN Ic 2003lw (*S20*), SN Ic 2004aw (*S19*), SN Ib 2005bf (*S8, S21*), and SN Ic 2006aj (*S22*).

**The Aspherical SN Model:**
The aspherical models presented in this paper are from (*S23, S24*). The jet-driven explosion is simulated by promptly depositing the kinetic and thermal energy in the innermost core. The initial kinetic energy is distributed in a jet-like way, applying $v_z = \alpha z$ and $v_r = \beta r$, where ($r$, $z$) is a cylindrical coordinate system (assuming axial symmetry with respect to the $z$-axis), and $v_z$ and $v_r$ are the initial deposited velocity components. Models BP8 and BP2 assume $\alpha/\beta$ = 8 and 2, respectively; see (*S23, S24*) for details. The distributions of density, $^{56}$Ni, and $^{16}$O are shown in Figure S1.

The optical depth to the [O I] $\lambda$6300 can be approximated by $0.01 M_{\rm O}/M_\odot (t_{\rm exp}/200\ {\rm days})^{-2}$ for a homogeneous medium with an oxygen mass of $M_{\rm O}$ and an expansion velocity of $0.02c$ (where $t_{\rm exp}$ is time since the explosion) (*S25*). The [O I] $\lambda$6363 line is always more transparent than the 6300 Å component because the latter has a larger transition probability.

Thus, the effect of the optical depth to the [O I] line profile should be negligible. Furthermore, we have confirmed that the [O I] line is always transparent in our models at $t_{\rm exp} > 200$ days. In this optically thin case, the blue (6300 Å) component is stronger than the red (6363 Å) one by a factor of 3, and the doublet behaves like a single transition.

The jet-driven model predicts unique features in the [O I] profile (Figs. S1 and S2) (*S23, S24*). The SN ejecta kinematics are described by homologous expansion, $R = v(R)t_{\rm exp}$, where $R$ and $v(R)$ are respectively the radius (in a spherical coordinate) and the radial expansion velocity of a point in the ejecta. Non-radial velocity components should be negligible. The observed wavelength of a photon depends on the point from which it was emitted, as $\lambda = \lambda_0(1 - v_{||}/c)$, where $\lambda_0$ is the rest wavelength of the line, $v_{||}$ is the line-of-sight velocity toward the observer, and $c$ is the speed of light. Then, defining $d$ as the projection of $R$ onto the line of sight, it can be shown that $v_{||} = d/t_{\rm exp}$, and this is the same in a given plane perpendicular to the line of sight. This means that, in the late phase, all photons emitted at the same depth along the line-of-sight have the same wavelength. The wavelength of a photon emitted from the near/far side of the ejecta is detected as shorter/longer (blueshifted/redshifted). Thanks to these characteristics, and to the transparency of the ejecta, the late-time emission profile can be used to probe the density distribution of the emitting gas within the SN ejecta (the "SN scan"), just like Computerized Tomography scans the human body (the "CT scan"). The SN scan is shown in Figure S1 for observers along the $z$-direction and $r$-direction, respectively. The model prediction (BP8) for the [O I] profile is shown in Figures S1 and S2 as a function of the viewing angle ($\theta$).

If we view the bipolar supernova explosion from a direction close to the jet axis, most of the O-rich material is in the equatorial region, expanding in a direction perpendicular to the line of sight and producing a narrow-peaked [O I] emission profile (Fig. S2). The SN scan provides a monotonically increasing amount of O-rich material as one probes nearer the center of the SN, then a monotonically decreasing amount of O-rich material as one moves away from the center (Fig. S1). On the other hand, the [O I] line shows a double-peaked profile if viewed from near the equatorial direction. In this case, the SN scan results in an increasing amount of O-rich material as one moves from the observer to the edge of the inner hole of the O-rich disk, then a decrease toward the center of the SN, where the non-emitting hole occupies the largest area. The amount of O then again increases as one moves from the center to the edge of the hole on the other side, and subsequently it again decreases toward the receding side of the ejecta (Fig. S1). Thus, two characteristic Doppler-shifted emission peaks (blueshifted and redshifted) appear.

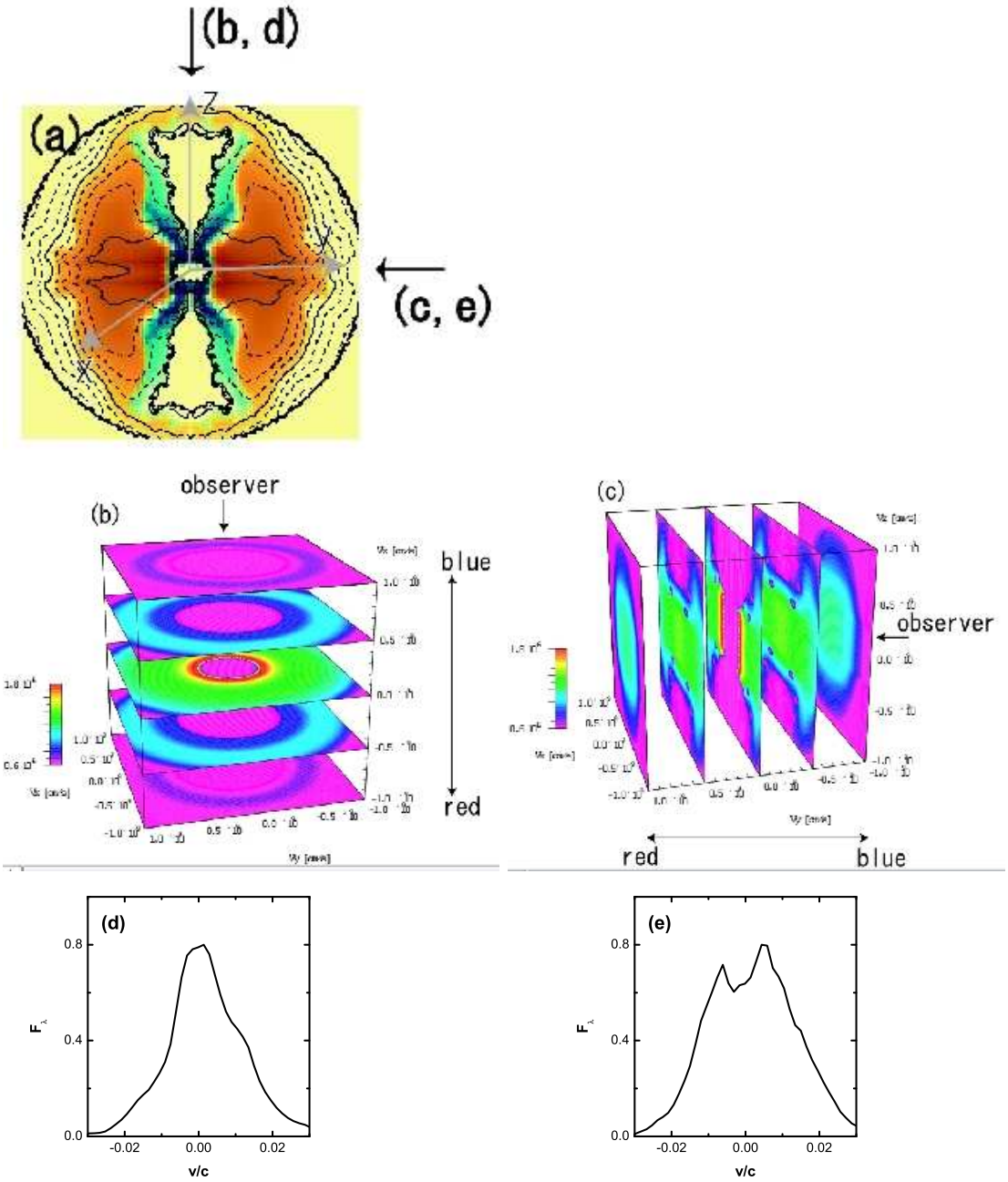


Figure S1: The bipolar Model BP8 (*S23, S24*). (a) Distribution of $^{56}$Ni (which decays into cobalt and then iron, shown in blue) and oxygen (red). Density contours are shown covering two orders of magnitude and divided into 10 equal intervals on a logarithmic scale. (b) The "SN scan" for the [O I] line as seen from an observer placed near the axis of the jet ($z$). (c) The SN scan for [O I] for an observer in the equatorial direction ($x-y$ plane). (d) The theoretical [O I] profile for an observer along the $z$-direction, and (e) along the equatorial direction.

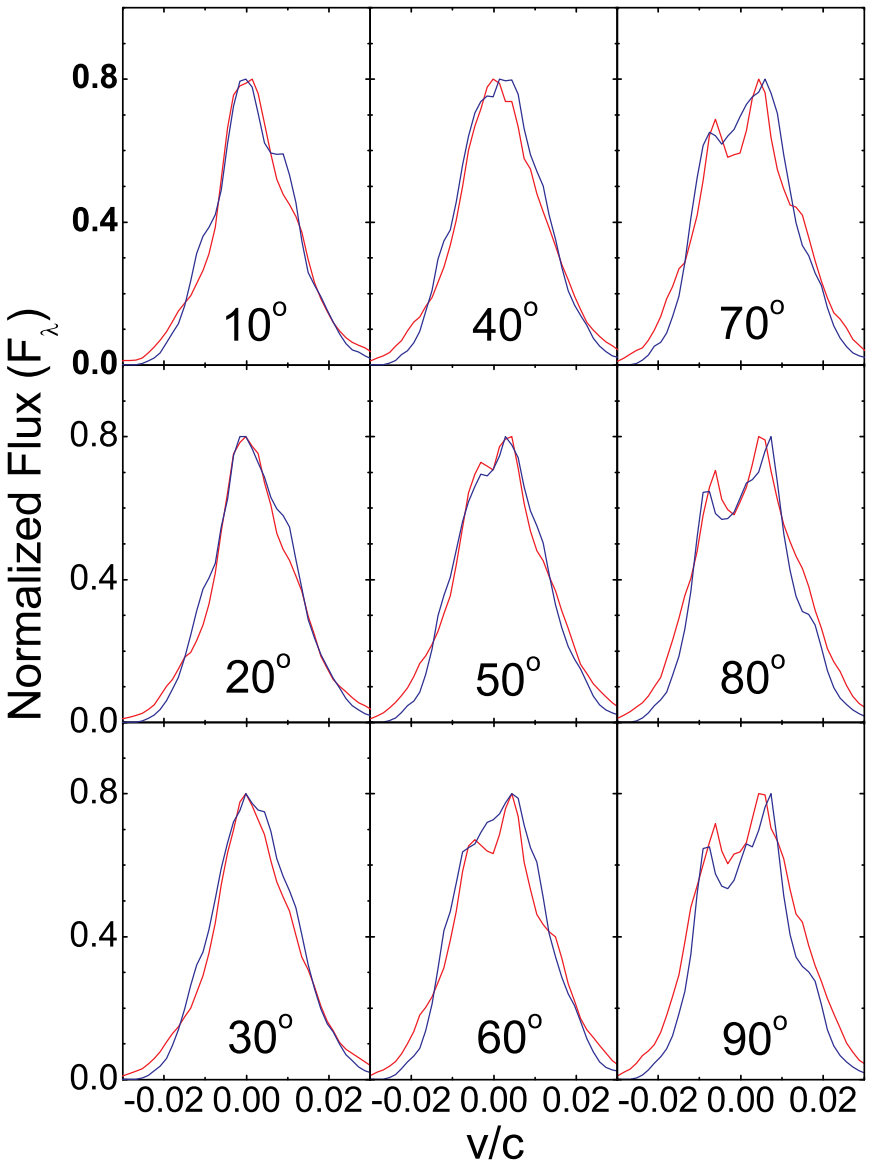


Figure S2: Predicted [O I] line profiles in the aspherical, jet-driven models BP8 (red) and BP2 (blue) as a function of the viewing angle $\theta$ (*S24*).

Table S1: Supernova Samples

| SN | Type | Observing Date | Days[1] | References | Figure[2] |
|---|---|---|---|---|---|
| 1991N | Ic | 1992-1-9 | 286 | Lick (*S1*) | ○ |
| 1997dq | broad-Ic | 1998-8-18 | 289 | Lick (*S1*) | ○ |
| 1997ef | broad-Ic | 1998-9-21 | 299 | Lick (*S1*) | ○ |
| 2002ap | broad-Ic | 2002-9-15 | 229 | Subaru (*S12*) | ○ |
| 2003jd | broad-Ic | 2004-9-12 | 323 | Subaru (*S11*) | ○ |
| 2004dk | Ib | 2005-7-6 | 342 | Subaru | |
| | | 2005-8-26 | 392 | Subaru | ○ |
| 2004fe | Ic | 2005-7-6 | 250 | Subaru | ○ |
| | | 2005-8-26 | 300 | Subaru | |
| 2004gk | Ic | 2005-7-6 | 224 | Subaru | ○ |
| 2004gn | Ic | 2005-7-6 | 218 | Subaru | ○ |
| 2004gq | Ib | 2005-8-26 | 258 | Subaru | |
| | | 2005-10-25 | 318 | Subaru | ○ |
| | | 2005-12-27 | 381 | Subaru | |
| 2004gv | Ib/c | 2005-7-6 | 206 | Subaru | |
| | | 2005-8-26 | 256 | Subaru | ○ |
| 2005aj | Ic | 2005-8-26 | 189 | Subaru | |
| | | 2005-10-25 | 249 | Subaru | |
| | | 2005-12-27 | 312 | Subaru | ○ |
| 2005kl | Ic | 2006-6-30 | 220 | Subaru | ○ |
| | | 2006-12-25 | 398 | Subaru | |
| 2005kz | broad-Ic | 2006-6-30 | 211 | Subaru | ○ |
| 2005nb | broad-Ic | 2006-6-30 | 195 | Subaru | ○ |
| | | 2007-1-24 | 403 | Subaru | |
| 2006F | Ib | 2006-6-30 | 173 | Subaru | |
| | | 2006-11-16 | 312 | VLT | ○ |
| 2006T | IIb | 2006-11-26 | 301 | Subaru | |
| | | 2006-12-25 | 329 | Subaru | ○ |
| | | 2007-2-18 | 384 | VLT | |
| 2006ck | Ic | 2007-1-24 | 249 | Subaru | ○ |

[1]Days since the discovery.
[2]The spectra shown in Figures 1 and 2 in the main text are marked by circles.

## References


S1. T. Matheson, A. V. Filippenko, W. Li, D. C. Leonard, & J. C. Shields, *Astron. J.* **121**, 1648 (2001).

S2. T. Nakamura, P. A. Mazzali, K. Nomoto, & K. Iwamoto, *Astrophys. J.* **550**, 991 (2001).

S3. Ph. Podsiadlowski, P. A. Mazzali, K. Nomoto, D. Lazzati, & E. Cappellaro, *Astrophys. J.* **607**, L17 (2004).

S4. K. Nomoto, et al., *Il Nouvo Cimento* **121B**, 1207 (2007) (astro-ph/0702472).

S5. E. Pian, et al., *Nature* **442**, 1011 (2006).

S6. F. Patat, et al., *Astrophys. J.* **555**, 900 (2001).

S7. G. Kosugi, et al., *Publ. Astron. Soc. Japan* **56**, 61 (2004).

S8. K. Maeda, et al., *Astrophys. J.* **666**, 1069 (2007).

S9. K. Maeda, et al., *Astrophys. J.* **658**, L5 (2007).

S10. P. A. Mazzali, et al., *Astrophys. J.* **661**, 892 (2007).

S11. P. A. Mazzali, et al., *Science* **308**, 1284 (2005).

S12. P. A. Mazzali, et al., *Astrophys. J.* **670**, 592 (2007).

S13. K. Maeda, P.A. Mazzali, & K. Nomoto, *Astrophys. J.* **645**, 1331 (2006).

S14. K. Nomoto, et al., *Nature* **364**, 507 (1993).

S15. D. N. Sauer, et al., *Mon. Not. R. Astron. Soc.* **369**, 1939 (2006).

S16. P. A. Mazzali, K. Iwamoto, & K. Nomoto, *Astrophys. J.* **545**, 407 (2001).

S17. P. A. Mazzali, et al., *Astrophys. J.* **572**, L61 (2002).

S18. P. A. Mazzali, et al., *Astrophys. J.* **599**, L95 (2003).

S19. S. Valenti, et al., *MNRAS* **in press** (2008).

S20. P. A. Mazzali, et al., *Astrophys. J.* **645**, 1323 (2006).

S21. N. Tominaga et al., *Astrophys. J.* **633**, L97 (2005).

S22. P. A. Mazzali, et al., *Nature* **442**, 1018 (2006).

S23. K. Maeda, et al., *Astrophys. J.* **565**, 405 (2002).

S24. K. Maeda, K. Nomoto, P. A. Mazzali, & J. Deng, *Astrophys. J.* **640**, 854 (2006).

S25. H. Li & R. McCray, *Astrophys. J.* **387**, 309 (1992).